



1 **Sources, fluxes, and behaviors of fluorescent dissolved organic matter (FDOM) in an**  
2 **estuarine mixing zone: Results from the Nakdong-River Estuary, Korea**

3

4 Shin-Ah Lee<sup>1</sup> and Guebuem Kim<sup>1\*</sup>

5 <sup>1</sup>School of Earth and Environmental Sciences/Research Institute of Oceanography, Seoul

6 National University, Seoul 08826, Republic of Korea

7

8

9

10

11

12

13

14

15 \*Corresponding author. Tel : +82-2-880-7508; Fax : +82-2-876-6508

16 E-mail address: gkim@snu.ac.kr (G.Kim)

17

18 Submitted to *Biogeosciences*



19    **Abstract**

20    We monitored seasonal variations of dissolved organic carbon (DOC), stable carbon isotope of  
21    DOC ( $\delta^{13}\text{C}$ -DOC), and fluorescent DOM (FDOM) in water samples from a fixed station in the  
22    Nakdong-River Estuary, Korea. Sampling was performed every hour during spring tide once a  
23    month from September 2014 to August 2015. The concentrations of DOC and FDOM showed  
24    significant negative correlations against salinity ( $r=0.55$ - $0.99$ ), indicating that the river-  
25    originated DOM components are the major source and behave conservatively in the estuarine  
26    mixing zone. The extrapolated  $\delta^{13}\text{C}$ -DOC values ( $-25.3\text{‰}$ ) in fresh water confirm that both  
27    components are mainly of terrestrial origin. The slopes of humic-like FDOM against salinity  
28    were 60-80% higher in the summer and fall, potentially due to higher fluvial production of  
29    humic-like FDOM. The slopes of protein-like FDOM against salinity, however, were 70-80%  
30    higher in spring, which could be due to higher biological production in river water. Our results  
31    suggest that there are large seasonal changes in riverine fluxes of humic and protein-like FDOM  
32    to the ocean.

33

34

35



## 1. Introduction

The global annual flux of dissolved organic carbon (DOC) via rivers is approximately  $0.17 - 0.36 \times 10^{15}$  g (Meybeck, 1982; Ludwig et al., 1996; Dai et al., 2012). The DOC delivered from riverine discharges as well as *in situ* production through biological activities significantly affects estuarine carbon and biogeochemical cycles in coastal waters (Hedges, 1992; Bianchi et al., 2004; Bauer et al., 2013; Moyer et al., 2015).

Generally, DOC includes fluorescent dissolved organic matter (FDOM), which emits fluorescent light due to its chemical characteristics (Coble, 2007). As FDOM accounts for 20 - 70% of DOC in coastal waters and controls the penetration of harmful UV radiation in the euphotic zone, it plays a critical role in carbon cycles as well as biological production. Additionally, FDOM is known to be a powerful indicator of humic and protein-like substances (Coble, 2007). River discharge is generally the main source of humic-like FDOM in coastal waters, although it is also produced through *in situ* microbial activity (Romera-Castillo et al., 2011). In contrast, the main sources of protein-like FDOM are biological production or anthropogenic sources (Baker and Spencer, 2004). Terrestrial humic substances behave conservatively in coastal areas due to their refractory characteristics (Del Castillo et al., 2000), whereas protein substances behave non-conservatively in many estuaries due to their relatively rapid production and degradation (Vignudelli et al., 2004).

The magnitudes of DOC and FDOM fluxes from rivers are known to be dependent on



rainfall, discharge, and temperatures (Maie et al., 2006; Jaffé et al., 2004; Huang and Chen, 2009). In the estuarine mixing zone, intensive biogeochemical processes occur through either photo-oxidation, microbial degradation or physicochemical transformations (i.e., flocculation, sedimentation) (Bauer and Bianchi, 2011; Moran et al., 1991; Benner and Opsahl, 2001; Raymond and Bauer, 2001). Recent studies have demonstrated large seasonal variations of DOC export from rivers to the ocean as high as 40% (Burns et al., 2008; Bianchi et al., 2004; Dai et al., 2012). However, the seasonal variations in sources, fluxes, and behaviors of DOC and FDOM in the estuarine mixing zone are still poorly understood.

65

In this study, we analyzed DOC,  $\delta^{13}\text{C}$ -DOC, and FDOM in estuarine water samples collected monthly from the Nakdong-River estuary. Sampling was conducted at a fixed platform, which has been utilized for monitoring various environmental parameters. This sampling station is advantageous as we can collect water samples of a wide range of salinity throughout tidal fluctuations. Using the data obtained from this unique station, we were able to determine (1) the behavior of DOM in the estuarine mixing zone, (2) the fluxes of DOM from rivers based on the slopes between salinity and DOM components, and (3) the changes of DOM sources using  $\delta^{13}\text{C}$ -DOC in estuarine samples. The slope measurement in the mixing zone represents the endmember of DOM components in rivers better than site specific measurements in the river.



## 76        **2. Materials and methods**

### 77        *2.1 Study site*

78                The Nakdong-River Estuary, which is the estuary of the longest river in Korea, is a  
79        major source of drinking, agricultural, and industrial supply water. The main channel of  
80        Nakdong River is approximately 510 km in length with an area of approximately 23,380 km<sup>2</sup>.  
81        It faces the south-eastern coastal area of the Korean peninsula, passing through Busan which  
82        is the second largest city in Korea. The mean annual precipitation is 1150 mm, and most  
83        precipitation (60-70%) occurs during the summer monsoon and typhoon seasons (Jeong et al.,  
84        2007). To manage water supply and saltwater intrusion, estuary dams were constructed in the  
85        mouth of the river in 1987.

86

### 87        *2.2 Sampling*

88                Water samples were collected at the sampling site which is located 560 m downstream  
89        from the dam (Fig. 1). The sampling period was from October 2014 to August 2015. The 2-L  
90        water sampling was conducted every hour for 24 hours during spring tide using an auto-sampler,  
91        with a depth the water intake 1 m below the surface. After samples were collected in acid-  
92        cleaned polyethylene bottles, they were moved to the laboratory within 24 hours. All water  
93        samples were filtered using pre-combusted GF/F filters. The FDOM samples were stored in  
94        pre-combusted amber glass vials and kept below 4°C in a refrigerator before analysis. The DOC  
95        and  $\delta^{13}\text{C}$ -DOC samples were acidified to pH ~2 using 6 M HCl, and stored in pre-combusted  
96        glass ampoules. Salinity was measured using a YSI Pro Series conductivity probe sensor in the  
97        laboratory. The real-time and compulsory discharge volume data from the dam are available at



98 <http://www.water.or.kr>, provided by K-Water.

99

### 100 *2.3 Analytical methods*

101 DOC concentration was determined by a high temperature catalytic oxidation (HTCO)  
102 method using a TOC-VCPH analyzer (Shimadzu, Japan). Standardization was performed based  
103 on the calibration curve of acetanilide in ultra-pure water. The acidified samples were purged  
104 with carbon dioxide (CO<sub>2</sub>) free carrier gas for 2 min to remove inorganic carbon. The samples  
105 were then injected into a combustion column packed with Pt coated alumina beads and heated  
106 to 720°C. The CO<sub>2</sub> evolving from combusted organic carbon was detected by a non-dispersive  
107 infrared detector (NDIR). Our DOC method was verified with seawater reference samples for  
108 DOC (44-46 μmol L<sup>-1</sup>) produced by the University of Miami, USA. They were consistent  
109 within 5%.

110

111 The values of δ<sup>13</sup>C-DOC were measured using a TOC-IR-MS instrument consisting  
112 of an IR-MS instrument coupled with a vario TOC cube (Isoprime, Elementar, Germany). The  
113 TOC instrument uses a common high-temperature catalytic combustion method (Kirkels et al.,  
114 2014). The analytical method is fully described in Kim et al. (2015). Briefly, 10 mL of filtered  
115 samples were purged with O<sub>2</sub> gas for 20–30 min to completely remove DIC after the samples  
116 were acidified to pH ~2. Then, 1 mL of the sample was injected into Pt-impregnated catalyst  
117 in a quartz tube. In this tube, the DOC was converted entirely to CO<sub>2</sub> at 750°C, which was then  
118 fed through a water trap followed by a halogen trap. After DOC was detected by an NDIR



119 detector, the CO<sub>2</sub> gas entered the TOC–IR–MS interface by the O<sub>2</sub> carrier gas. In the interface,  
120 the CO<sub>2</sub> was transferred to the IR–MS instrument following the removal of any interfering  
121 gasses. The  $\delta^{13}\text{C}$ -DOC value of blank was measured by low carbon water from Hansell lab  
122 (University of Miami), which contains less than 2  $\mu\text{M}$  DOC. Certified IAEA-CH6 sucrose  
123 (International Atomic Energy Agency,  $-10.45 \pm 0.03\text{‰}$ ) prepared with the low carbon water  
124 was used as a standard solution. Standard sample was analyzed at every sample queue (once  
125 before or after ten samples) to identify a drifting effect during measurements. The blank  
126 correction was performed using a method previously described in De Troyer et al. (2010) and  
127 Panetta et al. (2008). Our measurement result of  $\delta^{13}\text{C}$ -DOC for the Deep-Sea Water Reference  
128 (University of Miami) was  $-21.5 \pm 0.1\text{‰}$ , which is consistent with the results reported by  
129 Panetta et al. (2008) and Lang et al. (2007). The reproducibility of TOC–IR–MS was  $\sim 0.3\text{‰}$ .

130

131 FDOM fluorescence was determined in a scan mode using a spectrofluorometer  
132 (SCINCO FluoroMate FS-2) within two days after sampling. Emission (Em) spectra were  
133 collected from 250 to 600 nm at 2 nm intervals at excitation (Ex) wavelengths from 250 nm to  
134 500 nm at 5 nm intervals. Daily fresh distilled water backgrounds were subtracted from the  
135 sample data to eliminate Raman Scatter peaks (Zepp et al., 2004). All data were obtained in  
136 counts per second (cps), and converted to a ppb quinine sulfate standard solution in 0.1 N  
137 sulfuric acid at Ex/Em of 350/450 nm. EEMs-PARAFAC analysis was performed using a  
138 MATLAB R2013a program with a DOMFluor toolbox. The analyses identified two main  
139 components in all the samples collected in this study (humic-like component: FDOM<sub>H</sub>, protein-  
140 like component: FDOM<sub>P</sub>).



141

### 142       **3. Results and Discussion**

143               Salinities ranged from 0.1 to 28.5 over the sampling period of a year. Salinities in the  
144       sampling location were primarily dependent on the volume of river water discharge from the  
145       dam. The volumes of river discharge were larger in October, April, July, and August. The mean  
146       annual surface water temperature was 16°C, with the lowest temperature (avg. 8°C) in  
147       December and the highest temperature in August (avg. 26°C).

148

#### 149       *3.1 Behavior and sources of DOC in the estuarine mixing zone*

150               The concentrations of DOC ranged from 100 to 300 µM, with the highest  
151       concentrations in July (avg. 243 µM) and the lowest in February (avg. 115 µM), consistent with  
152       the typical DOC concentration ranges (Wang et al., 2004; Raymond and Bauer, 2001). The  
153       concentrations of DOC correlated significantly with salinity ( $r = 0.78-0.96$ ,  $p < 0.0001$ ),  
154       indicating that DOC behaves conservatively in the mixing zone of this estuary (Fig. 2A), which  
155       is commonly observed in estuarine mixing zones (Laane, 1980; Mantoura and Woodward, 1983;  
156       Del Castillo et al., 2000; Clark et al., 2002; Jaffé et al., 2004).

157

158               If the high salinity periods are excluded, the slope of DOC versus salinity was higher  
159       in July and lower in May, which could be due to higher terrestrial DOC loading in the summer  
160       monsoon period, as observed in Horsens Fjord, Denmark (Markager et al., 2011) (Fig. 2). To  
161       determine the source of DOC in fresh water, we plotted  $\delta^{13}\text{C}$ -DOC values against salinity (Fig.





2B). Generally,  $\delta^{13}\text{C}$ -DOC values range from  $-18$  to  $-22\text{‰}$  for marine phytoplankton, from  $-23\text{‰}$  to  $-34\text{‰}$  for terrestrial C3 plants, and from  $-16\text{‰}$  to  $-10\text{‰}$  for terrestrial C4 plants (Gearing 1988; Clark and Fritz, 1997). The carbon isotope values in our plot are well fitted with the conservative mixing curve of  $\delta^{13}\text{C}$  value for the two end-member mixing equation (Spiker, 1980; Raymond and Bauer, 2001):

$$\delta^{13}\text{C}_s = \frac{F_r \delta^{13}\text{C}_r [\text{DOC}]_r + (1 - F_r) \delta^{13}\text{C}_m [\text{DOC}]_m}{[\text{DOC}]_s} \quad (1)$$

where  $\delta^{13}\text{C}_s$ ,  $\delta^{13}\text{C}_r$  and  $\delta^{13}\text{C}_m$  are the  $\delta^{13}\text{C}$ -DOC values at a given sample salinity, river, and marine endmember salinity, respectively;  $F_r$  is the riverine freshwater fraction calculated from salinity;  $[\text{DOC}]_s$ ,  $[\text{DOC}]_r$ , and  $[\text{DOC}]_m$  are the DOC concentrations at a given salinity, the river, and marine end-members, respectively.

The curve fit shows that the end-member value of DOC and  $\delta^{13}\text{C}$ -DOC approaches  $270 \mu\text{M}$  and  $-26\text{‰}$ , respectively, for the riverine freshwater end-member ( $S=0\text{‰}$ ) and  $100 \mu\text{M}$  and  $-19\text{‰}$ , respectively for the marine end-member ( $S=29\text{‰}$ ). These carbon isotope values confirm that the main source of DOC in the estuarine mixing zone is consistently from terrestrial C3 plants during all seasons.

### 3.2 Behavior and sources of FDOM in the estuarine mixing zone

The concentrations of  $\text{FDOM}_H$  ranged from 2.4 to 19.7 quinine sulphate unit (QSU), with the highest concentrations in July (avg.  $17.6 \mu\text{M}$ ) and the lowest in June (avg.  $3.4 \mu\text{M}$ )



182 (Fig. 2C). The concentrations of FDOM<sub>P</sub> ranged from 0.6 to 22.4, with the highest  
 183 concentrations in March (avg. 15.1 QSU) followed by October (avg. 13.6 QSU) (Fig. 2D).

184

185 The concentrations of both FDOM were significantly correlated with salinity ( $r = 0.73$ -  
 186  $0.99$ ,  $p < 0.0001$  for FDOM<sub>H</sub> and  $r = 0.55$ - $0.98$ ,  $p < 0.0001$  for FDOM<sub>P</sub>), indicating that they are  
 187 conservative in the mixing zone (Fig. 2). The monthly slopes of FDOM<sub>H</sub> and FDOM<sub>P</sub> ranged  
 188 from  $-0.15$  to  $-0.59$  and  $-0.15$  to  $-0.71$ , respectively. The higher FDOM<sub>H</sub> slopes in July and  
 189 October are similar to the trend of DOC (Fig. 2C), however, the seasons (March, February and  
 190 April) in which higher FDOM<sub>P</sub> slopes occurred differ from those of DOC and FDOM<sub>H</sub>,  
 191 indicating that both FDOM components have different source inputs (Fig. 2D).

192

193 As such, there was a significant positive correlation between FDOM<sub>H</sub> and DOC  
 194 concentrations throughout all sampling periods ( $r^2 = 0.93$ ,  $p < 0.0001$ ) (Fig. 3A), suggesting that  
 195 the sources of FDOM<sub>H</sub> and DOC are mainly from terrestrially-driven DOM based on  $\delta^{13}\text{C}$ -  
 196 DOC values. As FDOM does not usually contribute to a major portion of DOC, a positive  
 197 correlation between FDOM and DOC has only been observed in specific areas, such as river-  
 198 estuarine systems (Del Vecchio and Blough, 2004; Coble, 2007). Stedmon et al., (2006)  
 199 demonstrate that stronger correlations are observed between DOC and FDOM, as humus  
 200 substances derived from terrestrial DOM are more colored than *in situ* produced DOM.  
 201 Generally, terrestrial DOM occurring in rivers mainly originates from plant decomposition and  
 202 leaf litter in the form of humic substances (Huang and Chen, 2009). Thus, higher FDOM<sub>H</sub>  
 203 slopes in October and November 2014, relative to the other periods, could be associated with



204 higher terrestrial inputs of organic weathering products in the fall (Dowell, 1985; Qualls et al.,  
 205 1991).

206

207 In the study region, FDOM<sub>P</sub> was poorly correlated with DOC concentrations ( $r^2=0.11$ )  
 208 (Fig. 3B). The slopes of FDOM<sub>P</sub> against DOC concentration varied significantly over different  
 209 seasons. The steeper gradients were observed in the spring (March and April) and fall (October),  
 210 and gradual gradient in the summer (July and August). In general, FDOM<sub>P</sub> is produced  
 211 efficiently by biological production in water (Coble, 1996; Belzile et al., 2002; Steinberg et al.,  
 212 2004; Zhao et al., 2017), thus, the higher FDOM<sub>P</sub> relative to DOC concentrations in the spring  
 213 and fall seems to be associated with the spring and fall phytoplankton blooms in this river  
 214 (Mayer et al., 1999; Zhang et al., 2009).

215

### 216 3.3 Fluxes of DOC and FDOM in the estuarine mixing zone

217 The fluxes of DOC and FDOM from rivers to the ocean were calculated using the  
 218 endmember values (C) of these components in rivers multiplied by the river discharge volumes  
 219 (Q) for each month (Fig. 4). For this estimation, we assumed that (1) the endmember values  
 220 were the same as the intercepts of the DOC, FDOM<sub>H</sub>, and FDOM<sub>P</sub> versus salinity plots, and  
 221 (2) the endmember values measured in the spring tides represent the concentrations of these  
 222 components for each month.

223

224 River discharge was highest in April and July following heavy precipitation, and the



largest discharge volume was about five-fold higher than that of winter discharges (Fig. 4A). However, the monthly variations of DOC endmember (y-intercept) values were quite constant, ranging from 174 - 284  $\mu\text{M}$ . This indicates that the concentrations of DOC in the river are independent of river discharge volumes (Fig. 4B). The DOC endmember values were the highest in December, followed by July and June (Fig. 4B). The monthly variation trend of  $\text{FDOM}_\text{H}$  endmember values was similar to that of DOC, except December value, which has a large uncertainty owing to the narrow, high salinity range of the samples collected. Excluding December value, the  $\text{FDOM}_\text{P}$  endmember values were highest in March, February, and October. These endmember trends are consistent with the slope variations explained in the previous section. Although these endmember values have large uncertainties for high salinity ranges in the winter, their contributions to the flux trend would be relatively small as discharge volumes were relatively small during these periods.

237

The riverine DOC flux ranged from  $1.6 \times 10^6 \text{ mol day}^{-1}$  in February to  $12.3 \times 10^6 \text{ mol day}^{-1}$  in July. The flux of DOC in July was about 8-fold larger than that in February, indicating that there are large variations of DOC fluxes to the ocean. Riverine flux of  $\text{FDOM}_\text{H}$  and  $\text{FDOM}_\text{P}$  ranged from  $1.4 \times 10^9 \text{ QSU m}^3 \text{ day}^{-1}$  (December) to  $23.1 \times 10^9 \text{ QSU m}^3 \text{ day}^{-1}$  (July) and from  $1.6 \times 10^9 \text{ QSU m}^3 \text{ day}^{-1}$  (June) to  $16.4 \times 10^9 \text{ QSU m}^3 \text{ day}^{-1}$  (March), respectively. The seasonal variation trend of  $\text{FDOM}_\text{H}$  was similar to that of DOC. The flux of  $\text{FDOM}_\text{H}$  in July was about 12-fold larger than that in February. The fluxes of  $\text{FDOM}_\text{P}$  in March and April were about 5-fold higher than those in February.

246



247 It is well known that the single sampling event is not enough to capture the full range  
248 of natural variability in DOM abundance over all seasons (Stedmon et al., 2006; Huang and  
249 Chen, 2009; Markager et al., 2011; Dai et al., 2012; Moyer et al., 2015). Overall, our results  
250 show that monthly variations are significant. This implies that our understanding of DOC  
251 fluxes from large rivers are largely biased, depending on sampling resolution. For example,  
252 summer data are extrapolated to annual river water discharge, the DOC and FDOM<sub>H</sub> fluxes can  
253 be overestimated up to 3 times.

254

#### 255 4. Conclusions

256 Large seasonal variations in the slopes of DOC, FDOM<sub>H</sub>, and FDOM<sub>P</sub> versus salinity  
257 were observed. The concentrations of FDOM<sub>H</sub> and DOC showed significant positive  
258 correlations with salinities throughout all sampling periods, indicating that they behave  
259 conservatively in this estuarine mixing zone. The slopes of both DOC and FDOM<sub>H</sub>  
260 concentrations versus salinity were higher in July, due to larger terrestrial DOC loading during  
261 the summer monsoon period. The carbon isotope values showed that the main source of DOC  
262 in the estuarine mixing zone is from terrestrial C<sub>3</sub> plants over all seasons. The slopes of FDOM<sub>P</sub>  
263 versus salinity were relatively higher in March and April in association with spring  
264 phytoplankton blooms in this river. The monthly fluxes of DOC, FDOM<sub>H</sub>, and FDOM<sub>P</sub> showed  
265 large seasonal variations (5-10 folds), suggesting that the estimation of annual riverine fluxes  
266 of DOC, FDOM<sub>H</sub>, and FDOM<sub>P</sub> requires careful considerations of seasonal changes in these  
267 components in rivers.

268



269 **Competing interests**

270 The authors declare that they have no conflict of interest.

271

272

273 **Acknowledgements**

274 We thank the Environmental and Marine Biogeochemistry Laboratory (EMBL)  
275 members for their assistance with sampling and laboratory analyses. This work was supported  
276 by the National Research Foundation of Korea (NRF) grant funded by the Korean government  
277 (MEST) (NRF-2015R1A2A1A10054309).

278

279 **References**

280 Baker, A., and Spencer, R. G.: Characterization of dissolved organic matter from source to sea  
281 using fluorescence and absorbance spectroscopy, *Sci. Total Environ.*, 333, 217-232, 2004.

282 Bauer, J., and Bianchi, T.: 5.02—dissolved organic carbon cycling and transformation, *Treatise*  
283 *on estuarine and coastal science*. Academic Press, Waltham, 7-67, 2011.

284 Bauer, J. E., Cai, W.-J., Raymond, P. A., Bianchi, T. S., Hopkinson, C. S., and Regnier, P. A.:  
285 The changing carbon cycle of the coastal ocean, *Nature*, 504, 61, 2013.

286 Belzile, C., Gibson, J. A., and Vincent, W. F.: Colored dissolved organic matter and dissolved  
287 organic carbon exclusion from lake ice: Implications for irradiance transmission and carbon  
288 cycling, *Limnol. Oceanogr.*, 47, 1283-1293, 2002.



- 289 Benner, R., and Opsahl, S.: Molecular indicators of the sources and transformations of  
290 dissolved organic matter in the Mississippi river plume, *Org. Geochem.*, 32, 597-611, 2001.
- 291 Bianchi, T. S., Filley, T., Dria, K., and Hatcher, P. G.: Temporal variability in sources of  
292 dissolved organic carbon in the lower Mississippi River, *Geochim. Cosmochim. Acta*, 68, 959-  
293 967, 2004.
- 294 Burns, K. A., Brunskill, G., Brinkman, D., and Zagorskis, I.: Organic carbon and nutrient fluxes  
295 to the coastal zone from the Sepik River outflow, *Cont. Shelf Res.*, 28, 283-301, 2008.
- 296 Clark, I.J., and Fritz, P.: *Environmental Isotopes in Hydrogeology*, CRC Press/Lewis Publishers,  
297 Boca Raton, 1997.
- 298 Clark, C. D., Jimenez-Morais, J., Jones, G., Zanardi-Lamardo, E., Moore, C. A., and Zika, R.  
299 G.: A time-resolved fluorescence study of dissolved organic matter in a riverine to marine  
300 transition zone, *Mar. Chem.*, 78, 121-135, 2002.
- 301 Coble, P. G.: Characterization of marine and terrestrial DOM in seawater using excitation-  
302 emission matrix spectroscopy, *Mar. Chem.*, 51, 325-346, 1996.
- 303 Coble, P. G.: Marine optical biogeochemistry: the chemistry of ocean color, *Chemical reviews*,  
304 107, 402-418, 2007.
- 305 Dai, M., Yin, Z., Meng, F., Liu, Q., and Cai, W.-J.: Spatial distribution of riverine DOC inputs  
306 to the ocean: an updated global synthesis, *Current Opinion in Environmental Sustainability*, 4,  
307 170-178, <https://doi.org/10.1016/j.cosust.2012.03.003>, 2012.
- 308 De Troyer, I., Bouillon, S., Barker, S., Perry, C., Coorevits, K., and Merckx, R.: Stable isotope  
309 analysis of dissolved organic carbon in soil solutions using a catalytic combustion total organic



- 310 carbon analyzer-isotope ratio mass spectrometer with a cryofocusing interface, *Rapid Commun.*  
 311 *Mass Spectrom.*, 24, 365-374, 2010.
- 312 Del Castillo, C. E., Gilbes, F., Coble, P. G., and Müller-Karger, F. E.: On the dispersal of  
 313 riverine colored dissolved organic matter over the West Florida Shelf, *Limnol. Oceanogr.*, 45,  
 314 1425-1432, 2000.
- 315 Del Vecchio, R., and Blough, N. V.: Spatial and seasonal distribution of chromophoric  
 316 dissolved organic matter and dissolved organic carbon in the Middle Atlantic Bight, *Mar.*  
 317 *Chem.*, 89, 169-187, 2004.
- 318 Dowell, W. H.: Kinetics and mechanisms of dissolved organic carbon retention in a headwater  
 319 stream, *Biogeochemistry*, 1, 329-352, 1985.
- 320 Gearing, J.N., The use of stable isotope ratios for tracing the nearshore–offshore exchange of  
 321 organic matter. In: Jansson, B.-O. (Ed.), *Coastal-Offshore Ecosystem Interactions*, Springer-  
 322 Verlag, Berlin, 69–101, 1988.
- 323 Hedges, J. I.: Global biogeochemical cycles: progress and problems, *Mar. Chem.*, 39, 67-93,  
 324 1992.
- 325 Huang, W., and Chen, R. F.: Sources and transformations of chromophoric dissolved organic  
 326 matter in the Neponset River Watershed, *Journal of Geophysical Research: Biogeosciences*,  
 327 114, 2009.
- 328 Jaffé, R., Boyer, J., Lu, X., Maie, N., Yang, C., Scully, N., and Mock, S.: Source  
 329 characterization of dissolved organic matter in a subtropical mangrove-dominated estuary by  
 330 fluorescence analysis, *Mar. Chem.*, 84, 195-210, 2004.





- 331 Jeong, K.-S., Kim, D.-K., and Joo, G.-J.: Delayed influence of dam storage and discharge on  
332 the determination of seasonal proliferations of *Microcystis aeruginosa* and *Stephanodiscus*  
333 *hantzschii* in a regulated river system of the lower Nakdong River (South Korea), *Water Res.*,  
334 41(6), 1269-1279.
- 335 Kim, T.-H., Kim, G., Lee, S.-A., and Dittmar, T.: Extraordinary slow degradation of dissolved  
336 organic carbon (DOC) in a cold marginal sea, *Sci. Rep.*, 5, 2015.
- 337 Laane, R.: Conservative behaviour of dissolved organic carbon in the Ems-Dollart estuary and  
338 the western Wadden Sea, *Neth. J. Sea Res.*, 14, 192-199, 1980.
- 339 Lang, S. Q., Lilley, M. D., and Hedges, J. I.: A method to measure the isotopic ( $^{13}\text{C}$ )  
340 composition of dissolved organic carbon using a high temperature combustion instrument, *Mar.*  
341 *Chem.*, 103, 318-326, 2007.
- 342 Ludwig, W., Probst, J. L., and Kempe, S.: Predicting the oceanic input of organic carbon by  
343 continental erosion, *Global Biogeochem. Cycles*, 10, 23-41, 1996.
- 344 Maie, N., Boyer, J. N., Yang, C., and Jaffé, R.: Spatial, geomorphological, and seasonal  
345 variability of CDOM in estuaries of the Florida Coastal Everglades, *Hydrobiologia*, 569, 135-  
346 150, 2006.
- 347 Mantoura, R., and Woodward, E.: Conservative behaviour of riverine dissolved organic carbon  
348 in the Severn Estuary: chemical and geochemical implications, *Geochim. Cosmochim. Acta*,  
349 47, 1293-1309, 1983.
- 350 Markager, S., Stedmon, C. A., and Søndergaard, M.: Seasonal dynamics and conservative  
351 mixing of dissolved organic matter in the temperate eutrophic estuary Horsens Fjord, *Estuarine*



- 352 Coastal Shelf Sci., 92, 376-388, 2011.
- 353 Mayer, L. M., Schick, L. L., and Loder, T. C.: Dissolved protein fluorescence in two Maine  
354 estuaries, Mar. Chem., 64, 171-179, 1999.
- 355 Meybeck, M.: Carbon, nitrogen, and phosphorus transport by world rivers, Am. J. Sci, 282,  
356 401-450, 1982.
- 357 Moran, M. A., Pomeroy, L. R., Sheppard, E. S., Atkinson, L. P., and Hodson, R. E.: Distribution  
358 of terrestrially derived dissolved organic matter on the southeastern US continental shelf,  
359 Limnol. Oceanogr., 36, 1134-1149, 1991.
- 360 Moyer, R. P., Powell, C. E., Gordon, D. J., Long, J. S., and Bliss, C. M.: Abundance,  
361 distribution, and fluxes of dissolved organic carbon (DOC) in four small sub-tropical rivers of  
362 the Tampa Bay Estuary (Florida, USA), Applied Geochemistry, 63, 550-562, 2015.
- 363 Panetta, R. J., Ibrahim, M., and Gélinas, Y.: Coupling a High-Temperature Catalytic Oxidation  
364 Total Organic Carbon Analyzer to an Isotope Ratio Mass Spectrometer To Measure Natural-  
365 Abundance  $\delta^{13}\text{C}$ -Dissolved Organic Carbon in Marine and Freshwater Samples, Anal. Chem.,  
366 80, 5232-5239, 2008.
- 367 Qualls, R. G., Haines, B. L., and Swank, W. T.: Fluxes of dissolved organic nutrients and humic  
368 substances in a deciduous forest, Ecology, 72, 254-266, 1991.
- 369 Raymond, P. A., and Bauer, J. E.: DOC cycling in a temperate estuary: a mass balance approach  
370 using natural  $^{14}\text{C}$  and  $^{13}\text{C}$  isotopes, Limnol. Oceanogr., 46, 655-667, 2001.
- 371 Romera-Castillo, C., Sarmiento, H., Álvarez-Salgado, X. A., Gasol, J. M., and Marrasé, C.: Net  
372 production and consumption of fluorescent colored dissolved organic matter by natural



- 373 bacterial assemblages growing on marine phytoplankton exudates, *Applied and environmental*  
374 *microbiology*, 77, 7490-7498, 2011.
- 375 Spiker, E.: The Behavior of C-14 and C-13 in Estuarine Water-Effects of Insitu Co<sub>2</sub> Production  
376 and Atmospheric Exchange, *Radiocarbon*, 22, 647-654, 1980.
- 377 Stedmon, C. A., Markager, S., Søndergaard, M., Vang, T., Laubel, A., Borch, N. H., and  
378 Windelin, A.: Dissolved organic matter (DOM) export to a temperate estuary: seasonal  
379 variations and implications of land use, *Estuaries and Coasts*, 29, 388-400, 2006.
- 380 Steinberg, D. K., Nelson, N. B., Carlson, C. A., and Prusak, A. C.: Production of chromophoric  
381 dissolved organic matter (CDOM) in the open ocean by zooplankton and the colonial  
382 cyanobacterium *Trichodesmium* spp, *Mar. Ecol. Prog. Ser.*, 267, 45-56, 2004.
- 383 Vignudelli, S., Santinelli, C., Murru, E., Nannicini, L., and Seritti, A.: Distributions of  
384 dissolved organic carbon (DOC) and chromophoric dissolved organic matter (CDOM) in  
385 coastal waters of the northern Tyrrhenian Sea (Italy), *Estuarine Coastal Shelf Sci.*, 60, 133-149,  
386 2004.
- 387 Wang, X.-C., Chen, R. F., and Gardner, G. B.: Sources and transport of dissolved and  
388 particulate organic carbon in the Mississippi River estuary and adjacent coastal waters of the  
389 northern Gulf of Mexico, *Mar. Chem.*, 89, 241-256, 2004.
- 390 Zepp, R. G., Sheldon, W. M., and Moran, M. A.: Dissolved organic fluorophores in  
391 southeastern US coastal waters: correction method for eliminating Rayleigh and Raman  
392 scattering peaks in excitation–emission matrices, *Mar. Chem.*, 89, 15-36, 2004.
- 393 Zhang, Y., van Dijk, M. A., Liu, M., Zhu, G., and Qin, B.: The contribution of phytoplankton



394 degradation to chromophoric dissolved organic matter (CDOM) in eutrophic shallow lakes:

395 field and experimental evidence, water research, 43, 4685-4697, 2009.

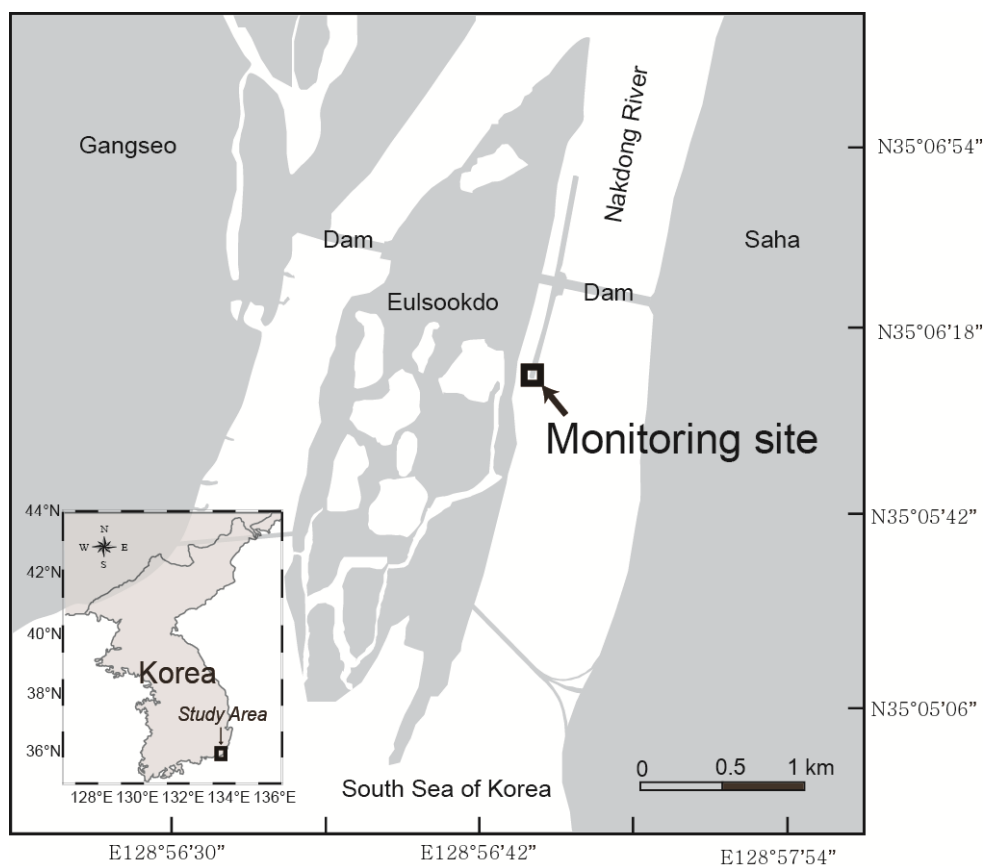
396 Zhao, Z., Gonsior, M., Luek, J., Timko, S., Ianiri, H., Hertkorn, N., Schmitt-Kopplin, P., Fang,

397 X., Zeng, Q., and Jiao, N.: Picocyanobacteria and deep-ocean fluorescent dissolved organic

398 matter share similar optical properties, Nature Communications, 8, 2017.

399

400



401

402 Figure 1 Map of Nakdong-River estuary. The square indicates a fixed monitoring site, located  
 403 560 m downstream from the dam.

404

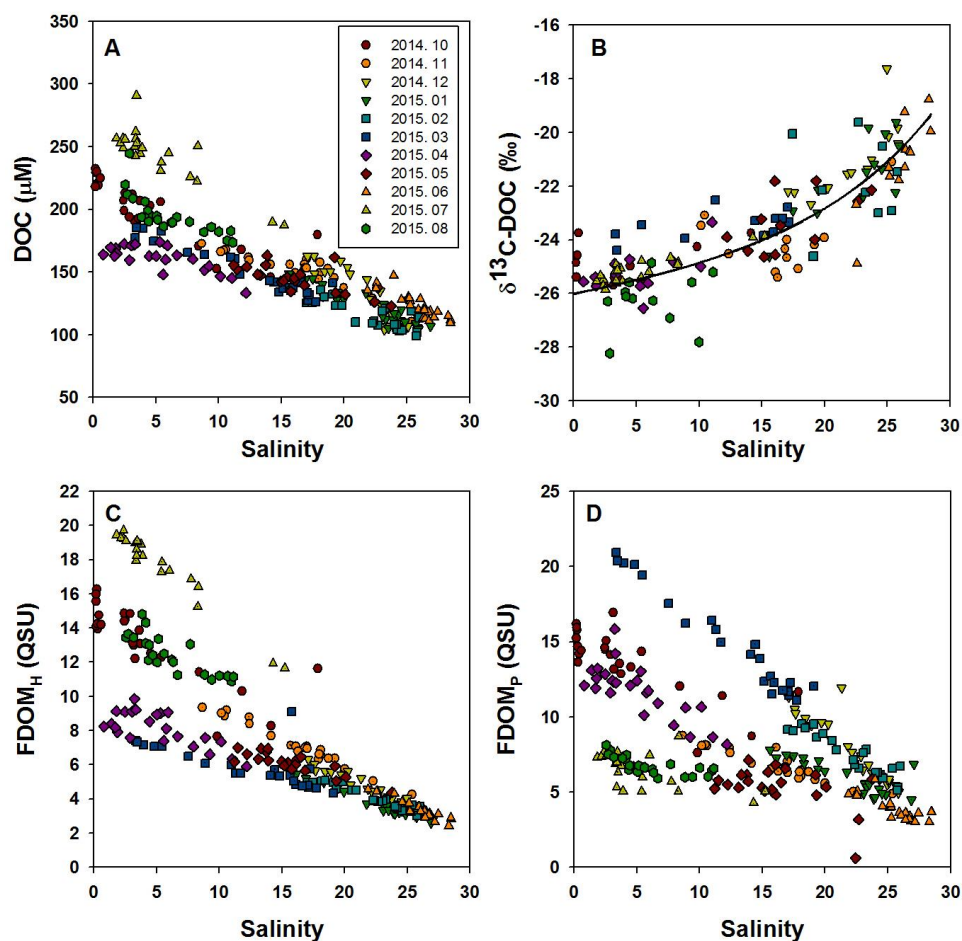
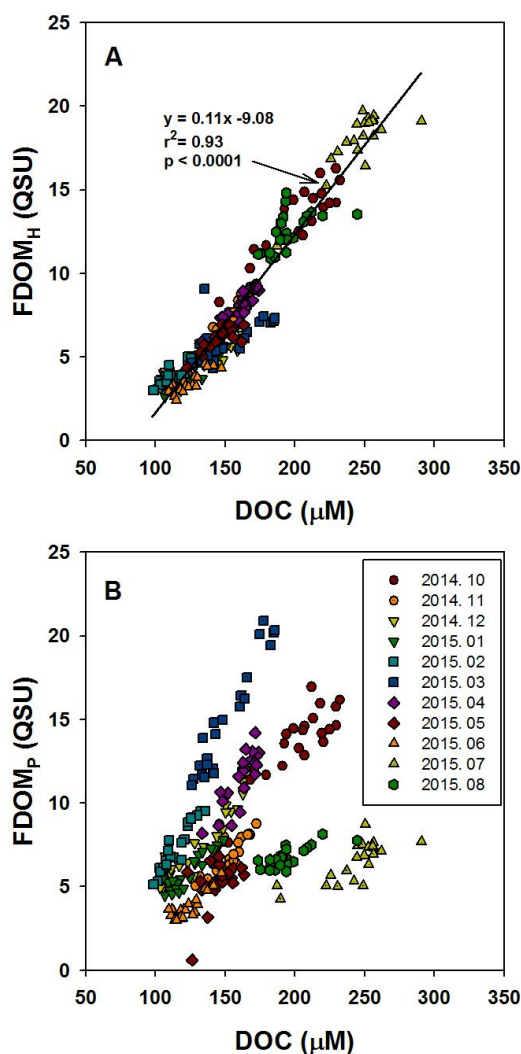


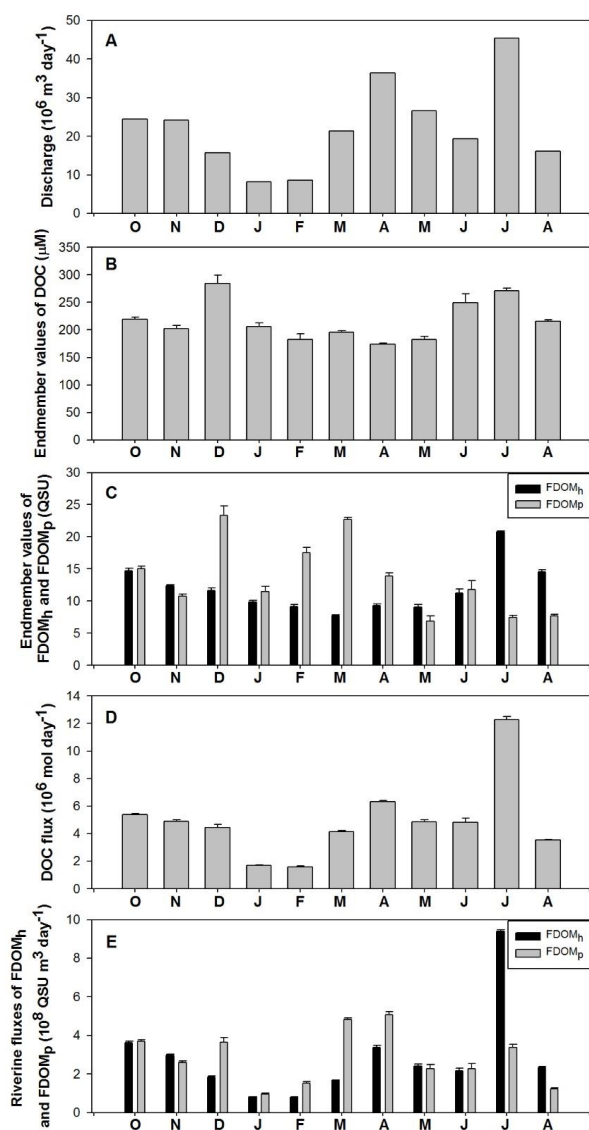
Figure 2 Salinity vs. (A) DOC, (B)  $\delta^{13}\text{C-DOC}$ , (C)  $\text{FDOM}_H$ , and (D)  $\text{FDOM}_P$ . The solid curve (B) is conservative mixing line for two end-member mixing equation.



409

410 Figure 3 DOC vs. (A) FDOM<sub>H</sub>, and (B) FDOM<sub>P</sub>. Solid line (A) is regression line and the slope  
 411 and  $r^2$  is shown.

412



413

414 Figure 4 Temporal variations of discharge, endmember values of DOC, FDOM<sub>H</sub>, and FDOM<sub>P</sub>,  
 415 and riverine fluxes of DOC, FDOM<sub>H</sub>, and FDOM<sub>P</sub> from October 2014 to August 2015.

416